Considerably long carrier lifetimes in high-quality 3C-SiC(111)

Jianwu Sun, Ivan Gueorguiev Ivanov, Rickard Liljedahl,
Rositsa Yakimova and Mikael Syväjärvi

Linköping University Post Print

N.B.: When citing this work, cite the original article.

Considerably long carrier lifetimes in high-quality 3C-SiC(111)

J. W. Sun (孙建武), I. G. Ivanov, R. Liljedahl, R. Yakimova, and M. Syväjärvi[a)]

Department of Physics, Chemistry and Biology, Linköping University, SE-58183, Linköping, Sweden

As a challenge and consequence due to its metastable nature, cubic silicon carbide (3C-SiC) has only shown inferior material quality compared with the established hexagonal polytypes. We report on growth of 3C-SiC(111) having a state of the art semiconductor quality in the SiC polytype family. The x-ray diffraction and low temperature photoluminescence measurements show that the cubic structure can indeed reach a very high crystal quality. As an ultimate device property, this material demonstrates a measured carrier lifetime of 8.2 μs which is comparable with the best carrier lifetime in 4 H-SiC layers. In a 760-μm thick layer, we show that the interface recombination can be neglected since almost all excess carriers recombines before reaching the interface while the surface recombination significantly reduces the carrier lifetime. In fact, a comparison of experimental lifetimes with numerical simulations indicates that the real bulk lifetime in such high quality 3C-SiC is in the range of 10–15 μs. © *2012 American Institute of Physics*. [http://dx.doi.org/10.1063/1.4729583]

During last two decades, silicon carbide has reached a semiconductor maturity as electronic material. Both 6H- and 4H-SiC materials are industrially produced, and high voltage devices have been commercialized based on these hexagonal SiC polytypes.[1,2] Although 3C-SiC would offer significant benefits over hexagonal SiC because of the high electron mobility, high-saturated electronic drift velocities, and isotropic properties,[3] it has not demonstrated comparable quality to the 6H and 4H-SiC polytypes. A major reason is its metastable phase formation, which makes it to form only at certain temperatures, and sensitivity to vapour phase composition. As a consequence, it cannot be grown by physical vapor transport (PVT) methods like applied for hexagonal SiC since 3C-SiC becomes less stable above 2000 °C. Only epitaxial growth with layers up to 200 μm by various methods is used.[4] Since 3C-SiC substrates are not available, the growth of 3C-SiC is usually done on either silicon substrates or hexagonal SiC substrates. The thermal and lattice mismatch using silicon substrates results in a large biaxial stress, which degrades the material properties.[5–7] The alternative way to achieve relaxed 3C-SiC is to use hexagonal SiC substrates.[4,8] However, the previous attempts to grow 3C-SiC layers have yielded inferior crystals with high densities of defects that hinders the implementation of its beneficial properties in electronic devices.[6] In addition, high quality 3C-SiC would be a perfect material for impurity based single cell photovoltaics with efficiency up to 60% (Ref. 9) since the bandgap is 2.4 eV and boron is a common acceptor dopant in SiC acting as a deep level at 0.7 eV.[10]

Carrier lifetime is one of the key parameters governing the electronic and optoelectronic device performance. It is very sensitive to the crystal quality. The carrier lifetime in 4H-SiC has been intensively investigated in recent years. Although 4H-SiC exhibits the highest maturity among all polytypes, the carrier lifetime is still short. The typical lifetime in as-grown 4H-SiC is around 1 μs under the low injection level.[11–16] The main lifetime-limiting defects are recognized as $Z_{1/2}$ and $EH_{6/7}$ centers, which are related to intrinsic defects with energy levels located at 0.65 eV and 1.55 eV below the conduction band, respectively.[11–14] Recently, it was shown that the reduction of the defects of $Z_{1/2}$ and $EH_{6/7}$ by post-growth processes results in an improvement of carrier lifetime. Kimoto *et al.*[15] reported that the carrier lifetime in a 148-μm-thick 4H-SiC layer is enhanced from 0.69 to 9.5 μs after thermal treatment. Miyazawa *et al.*[17] showed that using post carbon-implantation and annealing, the carrier lifetime in 4H-SiC was improved from 3.5 μs to an extraordinarily long value of 18–19 μs.

In contrast to 4H-SiC, the study of recombination dynamics in 3C-SiC is still limited due to the lack of high quality material.[18–21] In early 3C-SiC epitaxial layers with the thicknesses of 4–9 μm grown on silicon substrates, the excess carrier decay curves exhibited fast (a few μs) and slow (>1 ms) components, which was suggested to be due to electron trapping at deep defect levels.[18] It is not unexpected since the residual large strain results in a serious deterioration of the crystallinity and a defect-rich interface in such thin layers.[5–7] After the progress of different growth techniques in the last decade, free standing or thick (>100 μm) 3C-SiC has been demonstrated.[4] In these thick layers grown using either undulant Si,[19,20] or 4H-SiC,[19] or 6H-SiC as substrates,[20,21] however, the carrier lifetime is rather short. It is ranging from a few to 120 ns. These values are at least one order of magnitude lower than the lifetime in 4H-SiC.

In this work, we show that the crystal quality in extremely thick 3C-SiC grown by sublimation epitaxy is significantly improved compared with previous works. As a consequence, in as-grown 3C-SiC, a considerably longer carrier lifetime of 8.2 μs, which is comparable with the carrier lifetime in post growth treated chemical-vapor-deposition (CVD) grown 4H-SiC layers, is observed by microwave photoconductivity decay (μ-PCD) measurements. The experimental decay curves are also compared with the numerical simulations to resolve the impact of surface recombination and interface recombination on the carrier lifetime.

a)Email: mikael.syvajarvi@ifm.liu.se.

The 3C-SiC layers were grown on quarters of 6H-SiC substrates with area larger than 1 cm^2 by sublimation epitaxy.[22] The growth is performed by sublimation of a SiC source, and transport of the vapor species through vacuum to a substrate at lower temperature than the source. The growth is applied on substrates using a slight off-axis. In this mode, the 3C-SiC nucleates as domains, which extend in the off-axis direction and creates enlargement of domains. In the initial heating stage to growth temperature, the surface exhibits a thermal etching, which prepares the surface for growth and reduces effects of substrate polishing. In comparison to conventional PVT methods, the advantage of the method is that growth temperature is decreased to below 2000 °C at which 3C-SiC forms while high growth rate is maintained. Extremely thick layers (>300 μm) are obtained by modifying the process to reach a high growth rate, mainly by increasing the temperature difference between source and substrate. To explore surface and interface recombination, a very thick sample was grown as well during 45 min at a growth temperature of 1775 °C to reach a layer thickness of 760 μm. Low temperature photoluminescence (LTPL) spectra were measured at 2 K using the 351 nm line of an Ar$^+$-ion laser for excitation. The spectra are collected by a monochromator fitted with a 2400 grooves/mm grating in combination with a charge coupled device camera, with spectral resolution about 1 Å. High resolution x-ray diffraction (HR-XRD) measurements were performed using a Philips MRD with Cu Kα_1 ($\lambda = 1.54$ Å) radiation at 45 kV and 40 mA. The triple axis configuration was employed in the measurements by using a Ge (220) monochromator. The carrier lifetime was measured by μPCD at room temperature. The sample was excited using the 349 nm line of a frequency-tripled yttrium lithium fluoride laser with laser pulse of 5 ns. The laser penetration depth is 4.24 μm (absorption coefficient $\alpha = 2360$ cm^{-1}).[23] The injection level N$_0$, which was defined as the photon density illuminated on the sample surface per unit area, was varied from 3.5×10^{12} to 2.5×10^{13} cm^{-2} for the presented sample. Considering the penetration depth, the average excited carrier density N$_0\alpha$ is from 8.3×10^{15} to 5.9×10^{16} cm^{-3}. Thus, the injection levels in this study are very low but higher than the nitrogen doping level of around 1×10^{15} cm^{-3}, which was estimated from LTPL using an established procedure.[24]

The cubic sublimation method is applied at a temperature below 2000 °C. It was found that very high-quality 3C-SiC could be formed directly on 6H-SiC at a high growth rate of 1 mm/h. HR-XRD measurements were used to investigate the crystalline quality. In Figs. 1(a) and 1(b), x-ray incident angle (ω) scan rocking curves collected from (111) Bragg reflections for 3C-SiC with different foot print area on the sample evidence that single crystal domains have an average size of 0.6×0.6 mm^2. In larger foot print (2×2 mm^2) the peaks show a small splitting with the separation of 0.05°, which is due to several domains that are slightly off-oriented to each other. We measured HR-XRD by scanning the whole sample with step of 2 mm and the full width at half maximum (FWHM) values are between 50 and 100 arcsec with foot print of 2×2 mm^2. With decrease of the foot print to 0.6×0.6 mm^2, a single peak is observed having FWHM of 32 arcsec. As a comparison, commercial hexagonal substrates have values in the range of 25–40 arcsec.
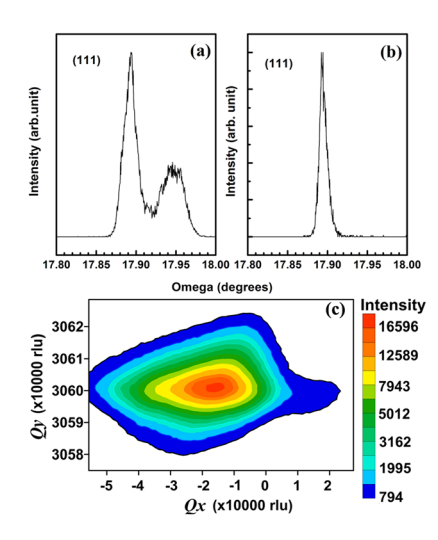

FIG. 1. HR-XRD ω scan rocking curves collected from (111) Bragg reflections for 3C-SiC with different foot print area: (a) 2×2 mm^2, (b) 0.6×0.6 mm^2. (c) XRD reciprocal space mapping with symmetric (111) reflection measured on 3C-SiC. This mapping reads the reciprocal scattering vector in reciprocal lattice unit (rlu) Qy(rlu) = 0.306003, which is used to calculate the lattice constant *a* value.

Reciprocal space mapping with symmetric (111) reflection has been performed on the sample to determine the lattice parameter.[25] From this mapping shown in Fig. 1(c), the lattice constant *a* is derived to be 4.3595 ± 0.0005Å, which is very close to the standard 3C-SiC *a* value of 4.3596 Å.[26] This unambiguously shows that the thick 3C-SiC grown on 6H-SiC has a negligible biaxial stress, which is the main reason that deteriorates the crystal quality of 3C-SiC grown on silicon substrates.

The LTPL spectrum demonstrates that the high-growth-rate sample exhibits a very high crystal quality. It is known that LTPL spectra in 3C-SiC are usually governed by the nitrogen bound no-phonon line (ZPL) and its four momentum-conserving phonon replicas (denoted TA, LA, TO, and LO).[27] In our samples, we found that the LTPL spectrum as seen in Fig. 2 is surprisingly distinct, especially compared to the LTPL spectra of CVD-grown 3C-SiC on silicon substrates:[5]

(i)   Only very sharp nitrogen-bound-exciton peaks without any defect-related emissions are observed. In 3C-SiC grown on silicon substrates, it usually shows broader nitrogen-bound-exciton peaks accompanied with defect-related emissions called "*W-band*" near 2.15 eV and "*G-band*" near 1.90–1.92 eV.[5] The LTPL does not exhibit any defect-related emissions or other residual impurity related emissions such as aluminum bound exciton and donor-acceptor-pair emissions. As shown in Fig. 2, the LTPL emission is very strong and the line width (FWHM) of the nitrogen-bound-exciton peak is rather narrow, around ~0.2 meV. In 3C-SiC, the width of the TA-phonon replica is sensitively proportional to the nitrogen doping concentration. From the FWHM value of TA line,[24] the nitrogen concentration in this 760-μm thick 3C-SiC can be estimated to be around 1×10^{15} cm^{-3}.

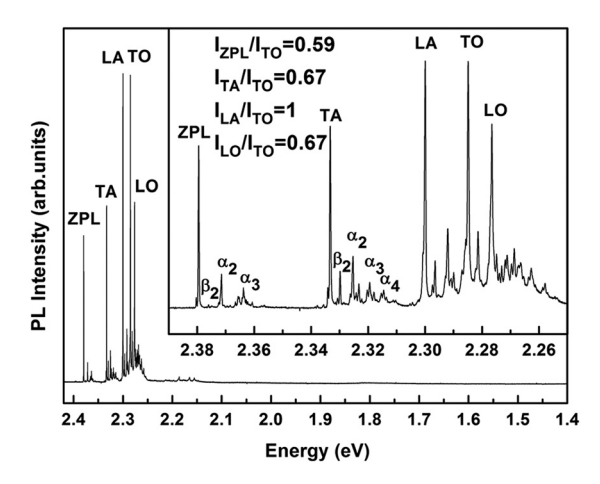(ii) It is known that the TO-phonon line is the strongest feature in 3C-SiC PL and seems not to be affected by

FIG. 2. Low temperature photoluminescence spectrum of the 760-μm thick 3C-SiC. The inset shows the enlarged part of the same spectrum from 2.25 to 2.39 eV, showing very sharp peaks with the full width at half maximum of 0.2 meV.

stress while the relative intensities of other phonon lines with respect to TO line largely depend on the biaxial stress. Consequently, the intensity ratio of LA mode to TO line (I_{LA}/I_{TO}) is used to evaluate the biaxial stress.[5] The typical value of I_{LA}/I_{TO} is around ~0.19 in 3C-SiC grown on Si substrate.[5] In contrast in our thick 3C-SiC, the ratio of I_{LA}/I_{TO} is equal to 1, indicating that the 760-μm thick 3C-SiC grown on 6H-SiC substrate is completely stress free. This agrees very well with the XRD results.

(iii) Besides the nitrogen-bound-exciton peaks, the multiple bound exciton complex lines are also well resolved. In this case, the nitrogen donor can bind m holes and $(m+1)$ electrons and one electron-hole pair can recombine and emit a photon.[28] We can clearly observe multiple bound exciton peaks up to $m=4$ (denoted by α_m). Additional fine lines (β_m) due to excited electron states were also observed.[28] Clearly, in order to bind more than one exciton at a nitrogen donor, a longer carrier lifetime (high quality material) is required; otherwise, the photo-generated carriers would quickly recombine before bounding more electron-hole pairs to the nitrogen donors ($m=2, 3, 4...$). Thus, these multiple bound excitons have been rarely observed in 3C-SiC and regarded as a characteristic of high-quality material.[29]

Notably, in agreement with the expectation of long carrier lifetime from LTPL observation of multiple bound excitons, we observed a considerably longer carrier lifetime in the 760-μm thick 3C-SiC by μ-PCD measurements. Fig. 3(a) shows μ-PCD decay curves measured at room temperature under different injection levels N_0 ranging from 3.5×10^{12} to 2.5×10^{13} cm^{-2}. All curves are non-exponential decays showing fast decay process at initial time stage and slow decay at the later stage. The initial fast decay is governed by surface recombination as discussed below.

The 1/e decay-times, which are defined as the time duration from the maximum of the peak after laser pulse illumination to 1/e of the peak, were extracted from μ-PCD curves and given in Fig. 3(b). It is apparent that the 1/e decay time decreases with increased injection level until $N_0 = 1.7 \times 10^{13}$ cm^{-2} is reached while further increasing
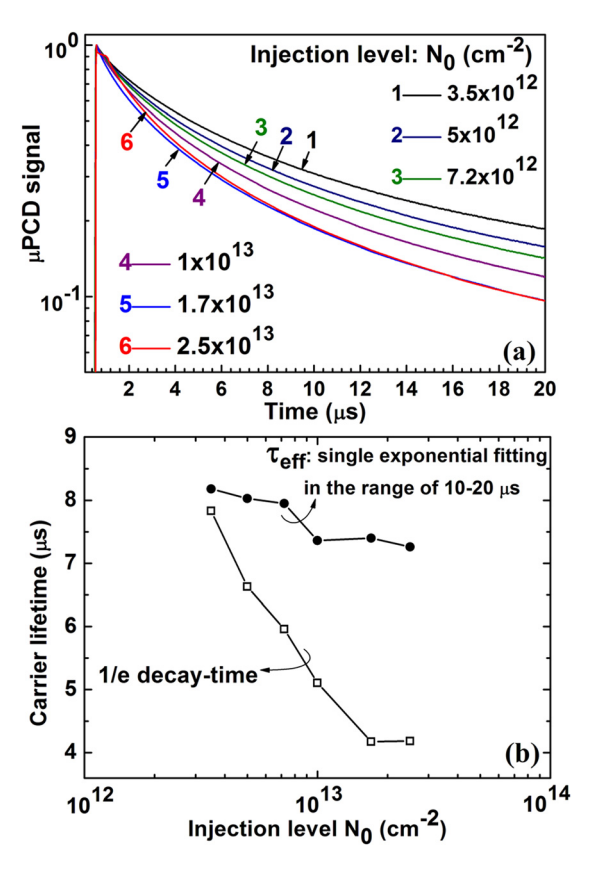

FIG. 3. (a) μ-PCD decay curve measured for the 760-μm thick 3C-SiC under different injection levels at room temperature. (b) The 1/e decay time and effective lifetime τ_{eff} as a function of injection level. τ_{eff} was obtained by the single exponential fitting in the range of 10–20 μs for μ-PCD curves.

injection level gives almost identical decays. This is not unexpected if taking the surface recombination into account. Considering the fact that the laser penetration depth (4.24 μm) is rather smaller with respect to the sample thickness (760-μm), we can only consider surface recombination velocity and neglect the interface recombination velocity. As we will see subsequently, the interface recombination indeed does not influence the excess carrier decay in such thick sample. It is known that carrier trapping at the surface states causes band bending near the surface, and one type of carriers is repelled from the surface, leading to reduced surface recombination velocity.[30] Such a band bending, however, depends sensitively on the injection carrier density and tends to flatten when the injection level increases. Therefore, surface recombination becomes significant, and the decay time is decreased with increasing the injection density until the surface band is flattened.

Since the surface recombination dominantly affects the initial decay process and thus results in a non-exponential decay curve, the effective lifetime should be determined by the fitting of the linear portion at slow stage where one should wait for the transient at least decay to about half of its maximum value.[31] As seen in Fig. 3(a), the portion of the decay curves in the range of 10–20 μs shows the intensity lower than 1/e of the peak value and can be fit by single exponential decay function very well. Thus, we extracted the effective lifetime τ_{eff} by the single exponential fitting in the range of 10–20 μs for μ-PCD curves. As shown in Fig. 3(b), the fitted τ_{eff} values decrease from 8.2 to 7.3 μs with

increasing the injection level, indicating that the surface recombination still gives a contribution at this time range but smaller than the impact in the initial stage. This measured carrier lifetime in as-grown 3C-SiC is much higher than the reported values in 3C-SiC grown by other methods,[19–21] even a little bit higher than the typical values in as-grown 4H-SiC.[11–15] The maximum carrier lifetime reported in as-grown 4H-SiC is 8.6 μs,[11] which was measured by μ-PCD in a high-quality 50 μm thick CVD epilayer under an injection of 5×10^{12} cm^{-2}. The measured conditions are quite similar to our measurements. The considerably longer lifetime clearly indicates a very high crystal quality of the 3C-SiC which is comparable with the best quality of CVD-grown thick 4H-SiC epilayers.

To further understand the influence of the surface and interface recombination on the carrier lifetime, we model the carrier dynamics for an n$^-$ 3C-SiC epilayer with very low doping concentration grown on a high-nitrogen doped n$^+$ 6H-SiC substrate under low injection conditions. The one dimensional continuity equation for the time dependent excess minority carrier concentration $\Delta p(z,t)$ is given by[13]

$$\frac{\partial \Delta p(z,t)}{\partial t} = D \frac{\partial^2 \Delta p(z,t)}{\partial z^2} - \frac{\Delta p(z,t)}{\tau_B}, \quad (1)$$

with boundary conditions

$$\left.\frac{\partial \Delta p(z,t)}{\partial z}\right|_{z=0} = S_1 \Delta p(0,t),$$

$$\left.\frac{\partial \Delta p(z,t)}{\partial z}\right|_{z=w} = -S_2 \Delta p(w,t).$$

The coordinate $0 \leq z \leq w$ indicates the depth axis of the epilayer with the thickness of $w = 760$ μm, D is the minority carrier diffusion coefficient, τ_B is the bulk carrier lifetime, S_1 is the surface recombination velocity, and S_2 is the interface recombination velocity. In the calculation, the injection level is fixed as same as the lowest value of $N_0 = 3.5 \times 10^{12}$ cm^{-2} used for μ-PCD measurement and D is assumed to be 3 cm^2/s,

which is the experimental value in 3C-SiC and 4H-SiC.[17,21]

Figs. 4(a)–4(c) show the depth profiles of the excess carrier concentration in the 760-μm thick layer as a function of time. In this case, the bulk lifetime was assumed to be a constant of 10 μs while the surface recombination velocity S_1 and interface recombination velocity S_2 are varied from 1 to 1×10^6 cm/s, independently. It is found that the interface recombination velocity S_2 actually does not give any contribution to the carrier distribution independent of the value of S_1, for instance, see a comparison of Figs. 4(a) and 4(b). It is apparent that almost all excess carriers are distributed in a depth of around 400 μm from the surface and cannot reach the interface. Hence, the generated carriers are annihilated through two pathways: surface recombination and bulk recombination.

Hereafter we will keep a constant of $S_2 = 1 \times 10^6$ cm/s. Two representative profiles with $S_1 = 1 \times 10^6$ cm/s and $S_1 = 1$ cm/s are compared in Figs. 4(a) and 4(c). Clearly, surface recombination velocity S_1 largely influences the distribution of excess carriers. In the case of enhanced $S_1 = 1 \times 10^6$ cm/s, the carrier concentration decreases abruptly near the surface. To illustrate the impact of enhanced S_1 on the carrier lifetime, we plot the decay curves of normalized excess carrier concentration $\Delta p(t)/\Delta p(0)$ by integrating excess carriers over the entire layer in Fig. 4(d). In this case, a carrier lifetime of 10 μs was used for the bulk lifetime, and S_1 was varied from 1 to 1×10^6 cm/s. It is clear that the decay curves almost follow a single exponential decay for small S_1 values while the increase of S_1 results in more and more faster decay at initial time region and gives non-exponential decays similar to those observed experimentally. For the same reason discussed above, the effective lifetimes τ_{eff} shown in Fig. 4(d) were also extracted by the single exponential fitting in the range of 10–20 μs for these calculated decay curves. For example, the effective lifetimes are very close to the bulk lifetime of 10 μs when $S_1 < 100$ cm/s while the enhanced surface recombination velocity significantly reduces the effective lifetime to 6.50 μs when $S_1 > 1 \times 10^5$ cm/s.
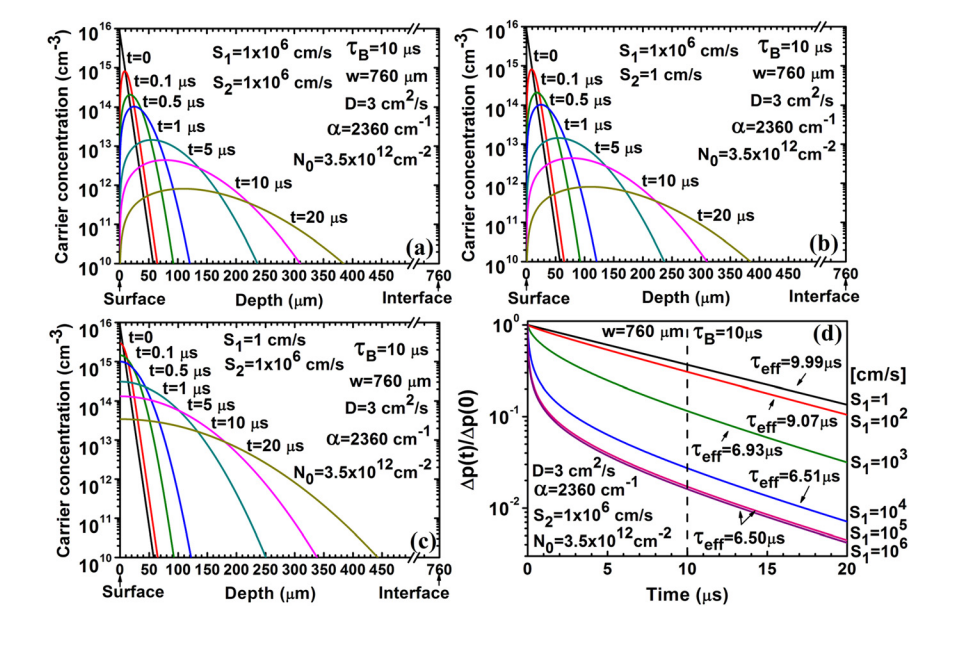

FIG. 4. Numerical simulated depth profiles of the excess hole concentration in a 760-μm thick 3C-SiC as a function of time with (a) $S_1 = S_2 = 1 \times 10^6$ cm/s, (b) $S_1 = 1 \times 10^6$ cm/s and $S_2 = 1$ cm/s, (c) $S_1 = 1$ cm/s and $S_2 = 1 \times 10^6$ cm/s. (d) The calculated decay curves of integrated excess carriers $\Delta p(t)/\Delta p(0)$ in the entire layer with S_1 changing from 1 to 1×10^6 cm/s. The effective lifetimes τ_{eff} shown in Fig. 4(d) were extracted by the single exponential fitting in the range of 10–20 μs.

Fig. 5 shows the effective lifetimes for the calculated decay curves as a function of surface recombination velocity S_1. In this calculation, the bulk lifetime was assumed to be 10, 15, and 20 μs, respectively, and the effective lifetimes were also obtained by the single exponential fitting for the calculated decay curves in the range of 10–20 μs. When S_1 is less than 100 cm/s, the effective lifetime is close to the bulk lifetime while it is significantly reduced with increase of S_1 until 1×10^4 cm/s and then becomes constant if $S_1 > 1 \times 10^4$ cm/s. As seen in Fig. 3, from μ-PCD decay curves measured on the 760-μm thick 3C-SiC, the effective lifetimes were decreased from 8.2 to 7.3 μs with increasing the injection level, namely, the increase of S_1. The dashed lines in Fig. 5 depict the range for these experimental lifetimes. Assuming the bulk lifetime is 20 μs, the lowest effective lifetime is 8.8 μs ($S_1 > 1 \times 10^4$ cm/s), which is still higher than the experimental data. This indicates that the bulk lifetime in this sample should be lower than 20 μs whatever the surface recombination velocity is. A comparison of experimental data with the calculated results suggests that the bulk lifetime in the 760-μm thick 3C-SiC should be in the range of 10–15 μs, assuming the surface recombination velocity S_1 is in a large range from a few hundreds to $\sim 10^4$ cm/s. Recently, the bulk carrier lifetime of 22–31 μs was evaluated in $\sim$265 μm thick 4H-SiC prepared using carbon-implantation and annealing treatment.[17] This indicates that our as-grown 3C-SiC has a comparable bulk lifetime to that of the post-growth treated 4H-SiC.

In conclusion, both the XRD and LTPL results reveal that the crystal quality of thick 3C-SiC is considerably improved with respect to earlier reported data. As a consequence, long carrier lifetime comparable with reported values in CVD-grown 4H-SiC is observed. A comparison of experimental lifetime with numerical simulations shows that the measured lifetime is significantly influenced by the surface recombination and the real bulk lifetime is estimated to
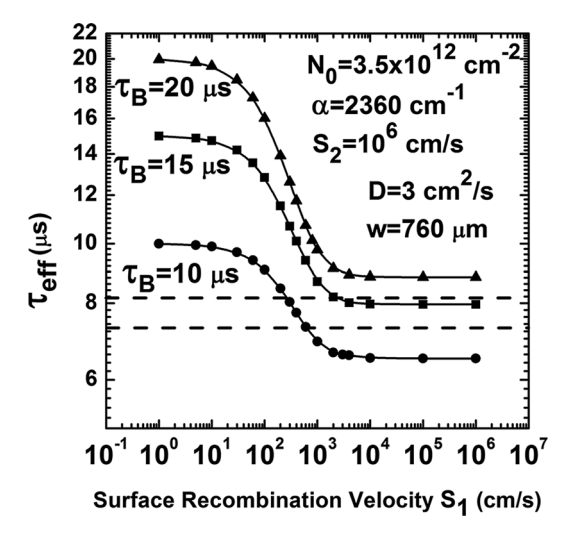
be in the range of 10–15 μs provided the surface recombination velocity is varied from a few hundreds to $\sim 10^4$ cm/s.

FIG. 5. The effective lifetimes τ_{eff} for the calculated decay curves as a function of the surface recombination velocity S_1. In this calculation, the bulk lifetime was assumed to be 10, 15, and 20 μs, respectively, and the effective lifetimes τ_{eff} were obtained by the single exponential fitting for the calculated decay curves in the range of 10–20 μs. The dashed lines show the experimental effective lifetime range of 8.2–7.3 μs measured by μ-PCD in the 760-μm thick 3C-SiC under injection level from 3.5×10^{12} to 2.5×10^{13} cm^{-2}.

[1] R. Rupp, M. Treu, A. Mauder, E. Griebl, W. Werner, W. Bartsch, and D. Stephani, Mater. Sci. Forum **338–342**, 1167 (2000).
[2] J. N. Shenoy, J. A. Cooper, Jr., and M. R. Melloch, Electron Device Lett. **18**, 93 (1997).
[3] A. Schöner, M. Krieger, G. Pensl, M. Abe, and H. Nagasawa, Chem. Vap. Deposition **12**, 523 (2006).
[4] See a recent review: G. Ferro, Mater. Sci. Forum **645–648**, 49 (2010).
[5] W. J. Choyke, Z. C. Feng, and J. A. Powell, J. Appl. Phys. **64**, 3163 (1988).
[6] E. Polychroniadis, M. Syväjärvi, R. Yakimova, and J. Stoemenos, J. Cryst. Growth **263**, 68 (2004).
[7] A. Galeckas, A. Yu. Kuznetsov, T. Chassagne, G. Ferro, J. Linnros, and V. Grivickas, Mater. Sci. Forum **457–460**, 657 (2004).
[8] R. Yakimova, G. R. Yazdi, N. Sritirawisarn, and M. Syväjärvi, Mater. Sci. Forum **527–529**, 283 (2006).
[9] G. Beaucarne, A. S. Brown, M. J. Keevers, R. Corkish, and M. A. Green, Prog. Photovolt: Res. Appl. **10**, 345 (2002); A. Luque and A. Marti, Phys. Rev. Lett. **78**, 5014 (1997).
[10] R. P. Devaty and W. J. Choyke, Phys. Status Solidi A **162**, 5 (1997).
[11] T. Kimoto, K. Danno, and J. Suda, Phys. Status Solidi B **245**, 1327 (2008).
[12] T. Hiyoshi and T. Kimoto, Appl. Phys. Express **2**, 041101 (2009).
[13] P. B. Klein, R. Myers-Ward, K.-K. Lew, B. L. VanMil, C. R. Eddy, Jr., D. K. Gaskill, A. Shrivastava, and T. S. Sudarshan, J. Appl. Phys. **108**, 033713 (2010).
[14] P. B. Klein, B. V. Shanabrook, S. W. Huh, A. Y. Polyakov, M. Skowronski, J. J. Sumakeris, and M. J. O'Loughlin, Appl. Phys. Lett. **88**, 052110 (2006).
[15] T. Kimoto, T. Hiyoshi, T. Hayashi, and J. Suda, J. Appl. Phys. **108**, 083721 (2010).
[16] L. Storasta, H. Tsuchida, T. Miyazawa, and T. Ohshima, J. Appl. Phys. **103**, 013705 (2008).
[17] T. Miyazawa, M. Ito, and H. Tsuchida, Appl. Phys. Lett. **97**, 202106 (2010).
[18] M. Ichimura, H. Tajiri, Y. Morita, N. Yamada, and A. Usami, Appl. Phys. Lett. **70**, 1745 (1997); M. Ichimura, N. Yamada, H. Tajiri, and E. Arai, J. Appl. Phys. **84**, 2727 (1998).
[19] P. Scajev, J. Hassan, K. Jarašiūnas, M. Kato, A. Henry, and J. P. Bergman, J. Electron. Mater. **40**, 394 (2011).
[20] V. Grivickas, G. Manolis, K. Gulbinas, K. Jarašiunas, and M. Kato, Appl. Phys. Lett. **95**, 242110 (2009).
[21] G. Manolis, K. Jarašiūnas, I. G. Galben, and D. Chaussende, Mater. Sci. Forum **615–617**, 303 (2009).
[22] M. Syväjärvi and R. Yakimova, "Sublimation epitaxial growth of hexagonal and cubic SiC," in *Encyclopedia—the Comprehensive Semiconductor Science & Technology (SEST)*, edited by P. Bhattacharya, R. Fornari, and H. Kamimura (Elsevier, 2011).
[23] S. G. Sridhara, T. J. Eperjesi, R.P Devaty, and W. J. Choyke, Mater. Sci. Eng. B **61–62**, 229 (1999).
[24] J. Camassel, S. Juillaguet, M. Zielinski, and C. Balloud, Chem. Vap. Deposition **12**, 549 (2006).
[25] J. Kräußlich, Anton J. Bauer, B. Wunderlich, and K. Goetz, Mater. Sci. Forum **353–356**, 319 (2001).
[26] A. Taylor and R. M. Jones, in *Silicon Carbide—A High Temperature Semiconductor*, edited by J. R. O'Connor, J. Smiltens (Pergamon, Oxford, 1960), p. 147.
[27] W. J. Choyke, D. R. Hamilton, and L. Patrick, Phys. Rev. **133**, A1163 (1964).
[28] J. P. Bergman, E. Janzen, and W. J. Choyke, Phys. Status Solidi B **210**, 407 (1998).
[29] L. Latu-Romain, D. Chaussende, C. Balloud, S. Juillaguet, L. Rapenne, E. Pernot, J. Camassel, M. Pons, and R. Madar, Mater. Sci. Forum **527–529**, 99 (2006).
[30] E. Yablonovitch, D. L. Allara, C. C. Chang, T. Gmitter, and T. B. Bright, Phys. Rev. Lett. **57**, 249 (1986).
[31] K. Schroder, *Semiconductor Materials and Device Characterization*, 3rd ed. (John Wiley & Sons, New York, 2006), Chap. 7.